

Angular dependence of magnetoresistivity in *c*-oriented MgB₂ thin film

C. Ferdeghini^{1,a}, V. Ferrando¹, V. Braccini¹, M.R. Cimberle², D. Marré¹, P. Manfrinetti³, A. Palenzona³, and M. Putti¹

¹ INFN-LAMIA, Dipartimento di Fisica, Via Dodecaneso 33, 16146 Genova, Italy

² IMEM/CNR, Dipartimento di Fisica, Via Dodecaneso 33, 16146 Genova, Italy

³ INFN, Dipartimento di Chimica e Chimica Industriale, Via Dodecaneso 31, 16146 Genova, Italy

Received 12 July 2002 / Received in final form 17 September 2002

Published online 29 November 2002 – © EDP Sciences, Società Italiana di Fisica, Springer-Verlag 2002

Abstract. The anisotropy of MgB₂ is still under debate: its value, strongly dependent on the kind of sample and on the measuring method, ranges between 1.2 and 13. In this work we present our results on MgB₂ *c*-oriented superconducting thin film. To evaluate the anisotropy, we followed two different approaches. Firstly, magnetoresistivity was measured as a function of temperature at selected magnetic fields applied both parallel and perpendicular to the *c*-axis; secondly, we measured magnetoresistivity at selected temperatures and magnetic fields, varying the angle θ between the magnetic field and the *c*-axis. The anisotropy estimated from the ratio between the upper critical fields parallel and perpendicular to the *c*-axis and the one obtained in the framework of the scaling approach within the anisotropic Ginzburg-Landau theory are different but show a similar trend in the temperature dependence. Some differences in the upper critical field and in its anisotropy of our film with respect to single crystals are emphasized: some of these aspects can be accounted for by an analysis of upper critical fields within a two-band model in presence of disorder and/or crystallographic strain.

PACS. 74.76.-w Superconducting films – 74.25.Fy Transport properties (electric and thermal conductivity, thermoelectric effects, etc.) – 74.60.Ec Mixed state, critical fields, and surface sheath

Introduction

The anisotropy is one of the still not clarified points in the newly discovered [1] superconductor MgB₂ and this topic is the object of a vivid debate. The anisotropy factor is usually defined as the ratio between the upper critical fields parallel and perpendicular to the basal planes: in the following we will call it $\gamma_{H_{C2}}$. $\gamma_{H_{C2}}$ seems to depend strongly on the kind of sample, on the measurement method, and on the criterion for defining the upper critical field. The data reported in the literature strongly depend on the kind of sample and on the measuring method and range between 1.2 and 13. Actually, high quality single crystals grown in boron nitrides crucibles now have reproducible properties and show consistent temperature dependent anisotropy values. They vary from 6 to 2.5 as the temperature increases from 4.2 to T_C [2–5]. This indicates that the anisotropy in the general absence of disorder is now well in hand. Different is the case of thin films in which the critical fields are strongly enhanced from the disorder and/or the crystallographic strain. Some H_{C2} values from literature both for thin films and single crystals [2–11] are collected in Figure 1. The critical

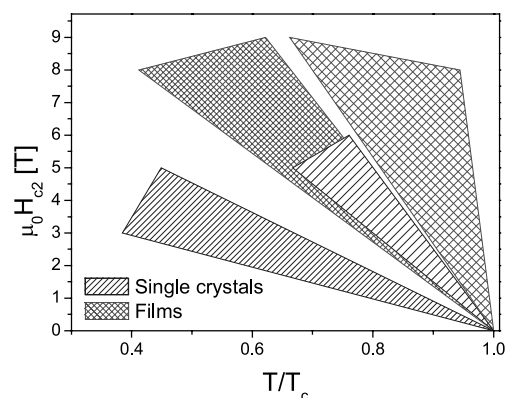


Fig. 1. $H_{C2}(\theta = 90^\circ)$ and $H_{C2}(\theta = 0^\circ)$ versus reduced temperature for thin films and single crystals [2–11].

fields for thin films are greater with respect to the single crystal ones in both directions but this difference is more marked when the field is perpendicular to the film surface. This behavior causes different values in the anisotropy factor: in the case of thin films $\gamma_{H_{C2}}$ ranges from 1.2 up to 3 [6–10] with the exception of [11] where a value 13 has been found on low T_C films. The fact that thin films

^a e-mail: Ferdeghini@fisica.unige.it

show less anisotropic behavior can be partially due to a not complete c -orientation, nevertheless the higher values and the different behavior in $H_{C2}(T)$ curves exhibited by thin films with respect to the single crystals suggest that some different physical mechanisms should play a role. In this paper we intend to study the critical field and the anisotropy in a well characterized thin film grown by a usual two-step technique. To evaluate its anisotropy we followed two different approaches. In the first, following the more usual procedure, magnetoresistivity measurements were performed as a function of temperature at selected magnetic field applied parallel and perpendicular to the c -axis, and $\gamma_{H_{C2}}$ was estimated. In the second, we measured magnetoresistivity at selected temperatures and magnetic fields varying the angle between the magnetic field and the c -axis; this latter approach, that takes into account the complete angular dependence of the upper critical field, is less affected by the presence of not aligned grains. We compare and discuss the obtained results and, in the light of the two-band nature of MgB_2 , we suggest the key role of disorder, strongly increased in thin films, in interpreting the great variety of apparently contradictory experimental results on MgB_2 anisotropy.

Sample preparation and characterization

The film was grown by means of Pulsed Laser Ablation by a standard two-step technique. The first step consisted in a room temperature high vacuum deposition of an amorphous precursor layer from MgB_2 sintered target [12]. An *ex situ* annealing in magnesium vapor is needed to crystallize the superconducting phase. Therefore, the sample was placed in a sealed tantalum tube with Mg lumps (approx 0.05 mg/cm^3) in Ar atmosphere, and then in an evacuated quartz tube and it was heated at $T = 850 \text{ }^\circ\text{C}$ for 30 minutes. A rapid quenching to room temperature followed this treatment. The choice of MgO in the (111) orientation was due to its hexagonal surface symmetry, like the one of MgB_2 , with a lattice mismatch smaller than 3%. X-ray diffraction measurements performed by synchrotron radiation at the ID32 beam line at the ESRF are reported in reference [8] and they indicate a dominant c -axis orientation: in the $\vartheta - 2\vartheta$ scans both the (001) and (002) reflections of the MgB_2 phase were outstanding with low intensity of the (101) reflection (the most intense reflection in randomly oriented powders). The rocking curve around the (002) reflection, showing a FWHM (Full Width at Half Maximum) of almost 1.3° , confirmed a good c -axis orientation. The sample did not show a single in-plane orientation: however, a strong azimuthal dependence was observed for the (100) reflection in X-rays grazing incidence measurements. The single in plane orientation is a quite difficult task for MgB_2 thin film and, only very recently, epitaxial films appeared in literature. [10,13,14]. The in-plane lattice parameter and the c -axis, calculated from the (100) reflection in grazing incidence measurements and from the (002) reflections measured in symmetrical configuration, turned out to be $a = 3.073 \text{ \AA}$ $c = 3.513 \text{ \AA}$, respectively. By comparing these values with those for MgB_2

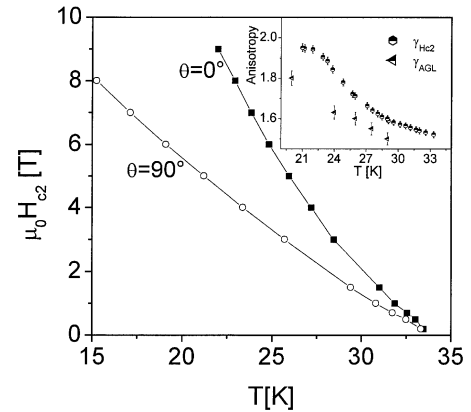


Fig. 2. $H_{C2}(\theta = 90^\circ)$ (open symbols) and $H_{C2}(\theta = 0^\circ)$ (full symbols) versus temperature. In the inset: $\gamma_{H_{C2}} = H_{C2}(\theta = 0^\circ)/H_{C2}(\theta = 90^\circ)$ (hexagons) as a function of temperature; γ_{AGL} (triangles) obtained from the best fit of $H_{C2}(\theta)$ with equation (1) (see text).

bulk ($a = 3.086 \text{ \AA}$ and $c = 3.524 \text{ \AA}$), we remarked that the sample is strained: the film adjusts the in-plane lattice with the hexagonal face of the substrate, so reducing the in-plane lattice parameter.

From resistivity measurements we found $T_C = 33.7 \text{ K}$, $\Delta T_C = 1 \text{ K}$, $\rho(40 \text{ K}) (\sim 100 \mu\Omega\text{cm})$ and the residual resistivity ratio $RRR = \rho(300 \text{ K})/(40 \text{ K}) = 1.5$. The $\rho(40 \text{ K})$ value is quite high, but agree with the typical values for thin films and it suggests that grain boundaries play an important role in the normal state transport properties of polycrystalline films. On the other hand, it was emphasized that, due to the large value of coherence length in MgB_2 , grain boundaries should not affect the intrinsic superconducting properties as the upper critical fields [15].

Experimental and discussion

Electrical resistance measurements were performed in a Quantum Design PPMS apparatus in applied magnetic field up to 9T by a four-probe AC resistance technique at 7 Hz. In order to study the anisotropy, we measured the resistance as a function of temperature, magnetic field, and angle θ between magnetic field and film surface. The current was always perpendicular to the magnetic field.

From the magnetoresistivity curves as a function of temperature, the upper critical field was estimated in the two directions (with the magnetic field parallel, $H_{C2}(\theta = 0^\circ)$, and perpendicular, $H_{C2}(\theta = 90^\circ)$, to the surface of the sample). The critical fields were evaluated at the point of the transition where the resistance is 90% of the normal state value. The results are shown in Figure 2, where the usual phase diagram with $H_{C2}(\theta = 0^\circ)$ values higher than $H_{C2}(\theta = 90^\circ)$ values is reported. In both directions (mainly for $\theta = 90^\circ$ the H_{C2} values are considerably higher in respect to single crystals ones (see Fig. 1). The two curves do not decrease linearly to zero but show a slight positive curvature, more evident in the upper curve

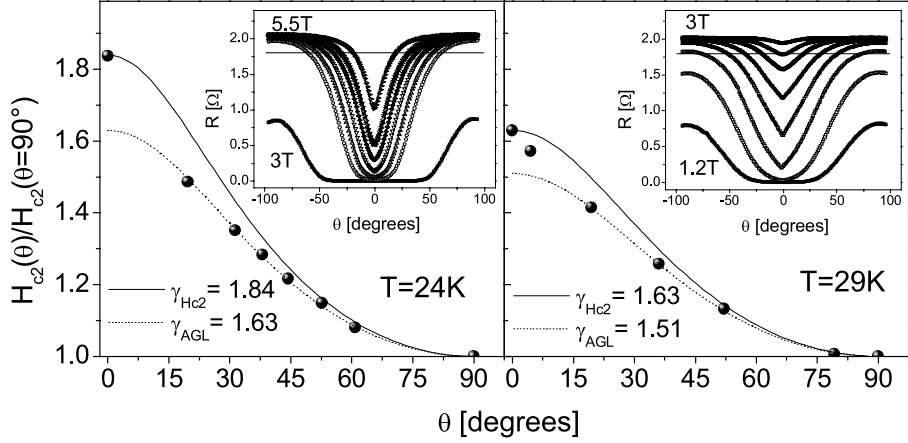


Fig. 3. Main panels: angular dependences of $H_{C2}(\theta)/H_{C2}(\theta = 90^\circ)$ for $T = 24$ K and $T = 29$ K; plot of equation (1) with $\gamma = \gamma_{H_{C2}} = 1.84$ ($T = 24$ K) and $\gamma = \gamma_{H_{C2}} = 1.63$ ($T = 29$ K) (continuous lines) and $\gamma = 1.63$ ($T = 24$ K) and $\gamma = 1.51$ ($T = 29$ K) (dashed lines). In the insets: magnetoresistivity as a function of the θ angle at $\mu_0 H = 3, 4, 4.25, 4.5, 4.75, 5, 5.5$ T for $T = 24$ K and at $\mu_0 H = 1.2, 1.4, 1.6, 1.8, 2, 2.25, 2.5, 3$ T for $T = 29$ K.

($H_{C2}(\theta = 0^\circ)$). The positive curvature of the upper critical field arises in the clean limit condition [16] and it is magnified in two-band anisotropic systems [17]. It is clearly observable in MgB₂ polycrystalline samples and single crystals, while in thin films it becomes less pronounced. Anyway a clear correlation between the progressive disappearing of the positive curvature and the decrease of RRR as been emphasized in thin films in [6, 8, 10]. This fact suggests that, in thin films also, the positive curvature is a signature of the clean limit establishment, irrespectively of the low RRR values due to the grain boundaries effect.

The anisotropy factor defined as $\gamma_{H_{C2}} = H_{C2}(\theta = 0^\circ)/H_{C2}(\theta = 90^\circ)$ is plotted in the inset of Figure 2. $\gamma_{H_{C2}}$ decreases from about 2 to 1.5, as temperature varies from 22 K to T_C . A similar temperature behavior of $\gamma_{H_{C2}}$ has been also observed in references [5] and [18]. We point out that these numbers must be managed with care because of the not perfect epitaxiality of the film that can imply a lower $H_{C2}(\theta = 0^\circ)$ value and, consequently, a $\gamma_{H_{C2}}$ underestimation. But the non-perfect alignments of the sample is no more a problem if a more sophisticated measurement technique is used, *i.e.* the H_{C2} angular dependence. In fact for high θ , when the applied magnetic field is far from parallelism with the film surface, the contribution of disoriented grains can be completely neglected.

The magnetoresistivity measurements as a function of the θ angle were performed with θ in the -100° – 100° range, at temperatures of 20, 24, 26, 27.5 and 29 K, and in magnetic fields up to 9 T. As an example, in the insets of Figure 3, two series of data acquired at 24 K and 29 K are plotted. As expected, all the curves show a pronounced minimum at $\theta = 0^\circ$: as the angle increases (in modulus), the resistivity increases and it reaches its maximum at $\theta = \pm 90^\circ$. From these curves the $H_{C2}(\theta)$ values can be calculated by drawing a horizontal line corresponding to 90% of the normal state resistivity value: the points where this line meets the magnetoresistivity curves give the $H_{C2}(\theta)$ values directly. In the main panels of Figure 3

the angular dependences of the so calculated $H_{C2}(\theta)$, normalized to $H_{C2}(\theta = 90^\circ)$, are reported for $T = 24$ K and 29 K; the values at $\theta = 0$ obviously correspond to $\gamma_{H_{C2}}$. No differences in the curves of Figure 2 are observed if the 50% of the normal state resistivity value is chosen as a criterion for the definition of $H_{C2}(\theta)$.

To interpret these experimental data we used the anisotropic Ginzburg-Landau (AGL) theory in which, in the effective mass tensor approximation, the angular dependence of the upper critical field is given by:

$$H_{C2}(\theta) = \frac{H_{C2}(\theta = 90^\circ)}{\left(\sin^2(\theta) + \frac{1}{\gamma_{AGL}^2} \cos^2(\theta)\right)^{1/2}} \quad (1)$$

where $\gamma_{AGL} = (M_c/M_{ab})^{1/2}$ is the ratio between the effective masses parallel (M_c) and perpendicular (M_{ab}) to the *c*-axis. It can be straightforwardly derived that $\gamma = H_{C2}(\theta = 0)/H_{C2}(\theta = 90^\circ) = \gamma_{H_{C2}}$. In Figure 3 equation (1) is plotted as a continuous line for $T = 24$ K and $T = 29$ K, with the same γ parameter previously calculated as the ratio of the critical fields ($\gamma_{H_{C2}}$) (and reported in the inset of Fig. 2). The continuous line does not fit the experimental data both at $T = 24$ K and 29 K, but it is possible to obtain a very good agreement with equation (1) by neglecting the low angle data, where a cuspid behavior is present and by using different γ values at different temperatures. The best fit curves for the experimental data for $\theta > 20^\circ$ are plotted as dashed lines in Figure 3. Although there are few data points for each curve, the best-fit procedure is accurate, equation (1) being quite sensitive to γ for values in the range 1–2. The data for $\theta < 20^\circ$, showing a cusp structure, lay above the dotted line. We point out that this behavior cannot be caused by a not perfect epitaxiality of the film: in fact, unaligned grains should cause a flattening rather than a cusp in the data. We underline that this cusp structure occurs whatever is the criterion chosen to define H_{C2} : the same γ_{AGL} values are obtained using the 50% of normal

state resistivity criterion for the H_{C2} determination. This fact indicates that, in our sample, surface superconductivity effect as suggested in [20] can be excluded.

A cusp structure for $H_{C2}(\theta)$ at $\theta = 0$ has been observed also in single crystals [19] by resistivity measurements. These authors also underlined that this behavior occurs whatever is the criterion chosen for the critical fields definition, as in our case. Always in single crystals, the $H_{C2}(\theta)$ values calculated from torque magnetometry, well follow equation (1) for all the angles [5] and also in [20] equation (1) is well followed when surface superconductivity effects are taken into account.

The new γ_{AGL} values are reported in the inset of Figure 2 as triangles; they show the same decreasing behavior with temperature as $\gamma_{H_{C2}}$, but they are 20% lower, ranging between 1.8 at 20 K and 1.5 at 29 K. This temperature dependence, as discussed in the following, is out of a simple AGL scheme.

In the AGL framework Blatter *et al.* [21] developed a general scaling approach that makes the treatment of the anisotropic behavior straightforward, at least on a formal basis. Within this model, apart from the region of low dissipation where disorder plays an important role, the resistivity data as a function of angle and magnetic field, if properly scaled, should collapse on the same curve. The rescaled functions are:

$$\tilde{\rho} = \rho \quad (2)$$

$$\tilde{H} = H \left(\sin^2(\theta) + \frac{1}{\gamma^2} \cos^2(\theta) \right)^{1/2}. \quad (3)$$

We verified the applicability of the scaling rules (2) and (3) on our $\rho(\theta, H)$ data and, for each temperature; we inserted the previously estimated γ_{AGL} parameter in \tilde{H} . The results are shown in Figure 4 for $T = 29$ K: the curves collapse all together on the measured $\rho(\theta = 90^\circ)$ versus magnetic field curve (continuous line). We mark that this occurs for all the levels of dissipation. Only the low angle data do not scale on the main curve, but they bend down with a sharper slope. This failure of the scaling at low angles, that we observed also in the angular dependence of the upper critical field, is a general feature occurring at all the temperatures. It can be explained within the scaling model [21]: in fact, in a layered superconductor the disorder within the planes and between adjacent planes will not be the same after rescaling, and the difference will be considerable in the small angle regime. This fact limits the applicability of the scaling to angles such that $|\theta| > \arctg(1/\gamma_{AGL})$. In our case this means $\theta > 25^\circ - 30^\circ$, which is the angular region we considered; this limit becoming less strict for larger anisotropies.

In the inset of Figure 4 we present $\tilde{\rho}$ as a function of \tilde{H} at $T = 20, 24, 26, 27.5$ and 29 K, without the low angle data. The scaling is quite good at all the investigated temperatures, even though it becomes less accurate when temperature decreases. Since at lower temperature the resistivity measurements are performed at higher magnetic fields, we cannot distinguish between the influence of the temperature and of the field.

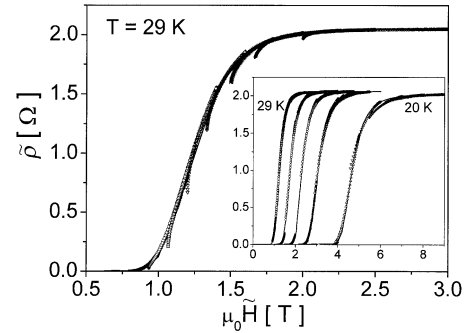


Fig. 4. $\tilde{\rho}$ versus \tilde{H} for $T = 29$ K: the plot shows the $\rho(\theta, H)$ data for ($\mu_0 H = 1.2, 1.4, 1.6, 1.8, 2, 2.25, 2.5, 3$ T scaled following the relationships (2) and (3); the curves collapse all together on the measured $\rho(\theta = 90^\circ, H)$ curve (continuous line). Inset: $\tilde{\rho}$ versus $\mu_0 \tilde{H}$ for $T = 20$ K ($\mu_0 H = 3, 4, 5, 6, 7, 8, 9$ T), $T = 24$ K ($\mu_0 H = 3, 4, 4.25, 4.5, 4.75, 5, 5.5$ T), $T = 26$ K ($\mu_0 H = 2, 3, 3.5, 4, 4.25, 4.5, 4.75$ T), $T = 27.5$ K ($\mu_0 H = 1.5, 2, 2.5, 2.75, 3, 3.25, 3.5, 3.75, 4$ T) and $T = 29$ K ($\mu_0 H = 1.2, 1.4, 1.6, 1.8, 2, 2.25, 2.5, 3$ T). Only the data for $\theta > 25^\circ$ are plotted.

In conclusion, the scaling procedure derived from the AGL approach, when it is applied in the case of MgB_2 , appears good enough for all the levels of dissipation, temperatures, and fields we tested and in the angular range predicted by the theory. But we found a temperature dependent anisotropic factor value, in contrast with the theory, at least in its basic form: we recall that this approach is developed for a single band anisotropic system.

In reference [22] Shulga and co-workers emphasized the necessity of considering a two-band model to account for the upper critical field behavior in MgB_2 . This model can qualitatively explain some features of the upper critical fields behavior. Generally, $H_{C2}(\theta = 0^\circ)$ shows a larger positive curvature than $H_{C2}(\theta = 90^\circ)$, which in some cases is simply linear (the monotone decrease of $\gamma_{H_{C2}}$ with temperature is a consequence of this fact). The two-band model [23] explains both the higher values and the more pronounced curvature of $H_{C2}(\theta = 0^\circ)$ as consequences of the strong anisotropy of the projection of the Fermi surface in the plane $\theta = 0^\circ$. Moreover in this framework the intra and inter-band scattering rates affect the upper critical field behavior [22] in a very complex way. Within this picture some differences between bulk and films can be explained in term of extra-scattering due to the presence of disorder and/or strain, strongly enhanced in films. In fact in weakly anisotropic two-band systems, H_{C2} behaves like in single band systems, increasing as disorder grows. On the contrary, in strongly anisotropic two-band systems, H_{C2} value decreases and the upward curvature is suppressed as the impurity content grows until the dirty limit is reached; then, a further increase in disorder causes an increase in H_{C2} . Because MgB_2 is isotropic in plane and anisotropic out-of-plane, we expect that disorder enhances $H_{C2}(\theta = 90^\circ)$ more than $H_{C2}(\theta = 0^\circ)$. This fact is confirmed by the literature data (see Fig. 1). The critical fields for thin films are greater with respect to the single crystal ones in both directions and this difference is more marked

for $H_{C2}(\theta = 90^\circ)$. This complex phenomenology explains why in thin films the anisotropy factor $\gamma_{H_{C2}}$ turns out to be smaller than in single crystals. So differences between these two kinds of systems can be ascribed mainly to the scattering with impurities, which is strongly enhanced in films.

Conclusions

We have studied the behavior of the upper critical fields and the anisotropy of a *c*-oriented thin film in two different ways: by the ratio between the critical fields perpendicular and parallel to the *c*-axis and by the angular dependence of magnetoresistivity at various fields and temperatures. The AGL theory well accounts for the angular dependence of magnetoresistivity in a large range of temperatures, magnetic fields and angles, and for all the level of dissipation. Nevertheless, a disagreement with the theory, which is based on the effective mass tensor approximation, appears in the temperature dependence of γ . Moreover, the AGL approach cannot take into account the very different anisotropy values reported in the literature, which seem to be related not to intrinsic properties but mainly to disorder.

We emphasized some differences in the upper critical fields of our film in respect to single crystals: higher values of H_{C2} lower curvature near T_C , lower anisotropy, cusp like structure in the angular dependence. Some of these aspects can be accounted for by a qualitative analysis of upper critical fields within a two-band model in presence of disorder. Anyway, a more complex model, taking the anisotropic multi-band nature of this compound into account, should be developed; on the other hand reliable data on epitaxial thin films or single crystals with controlled amount of disorder, should be collected. In fact, to clarify the disorder role that seems to be essential to increase H_{C2} and decrease anisotropy (both these aspects are crucial for applications) is a very important task for future development.

References

1. J. Nagamatsu, N. Nakawaga, T. Muranaka, Y. Zenitani, J. Akimitsu, *Nature* **410**, 63 (2001)
2. M. Xu, H. Kitazawa, Y. Takano, J. Ye, K. Nishida, H. Abe, A. Matsushita, G. Kido, *Appl. Phys. Lett.* **79**, 2779 (2001)
3. S. Lee, H. Mori, T. Masui, Yu. Eltsev, A. Yamamoto, S. Tajima, *J. Phys. Soc. Jpn* **70**, 2255 (2001)
4. K.H.P. Kim, Jae-Hyuk Choi, C.U. Jung, P. Chowdhury, Min-Seok Park, Heon-Jung Kim, J.Y. Kim, Zhonglian Du, Eun-Mi Choi, Mun-Seog Kim, W.N. Kang, Sung-Ik Lee, Gun Yong Sung, Jeong Yong Lee, *Phys. Rev. B* **65**, 100510 (2002)
5. M. Angst, R. Puzniak, A. Wisniewski, J. Jun, S.M. Kazakov, J. Karpinski, J. Roos, H. Keller, *Phys. Rev. Lett.* **88**, 167004 (2002)
6. S. Patnaik, L.D. Cooley, A. Gurevich, A.A. Polyanskii, J. Jiang, X.Y. Cai, A.A. Squitieri, M.T. Naus, M.K. Lee, J.H. Choi, L. Belenky, S.D. Bu, J. Letteri, X. Song, D.G. Schlom, S.E. Babcock, C.B. Eom, E.E. Hellstrom, D.C. Larbalestier, *Supercond. Sci. Technol.* **14**, 315 (2001)
7. M.H. Jung, M. Jaime, A.H. Lacerda, G.S. Boebinger, W.N. Kang, H.J. Kim, E.M. Choi, S.I. Lee, *Chem. Phys. Lett.* **243**, 447 (2001)
8. C. Ferdeghini, V. Ferrando, G. Grassano, W. Ramadan, E. Bellingeri, V. Braccini, D. Marre, M. Putti, P. Manfrinetti, A. Palenzona, F. Borgatti, R. Felici, C. Aruta, *Physica C* **378-381**, 56 (2002)
9. R. Vaglio, M.G. Maglione, R. Di Capua, *Supercond. Sci. Technol.* **15**, 1236 (2002)
10. V. Ferrando, S. Amoruso, E. Bellingeri, R. Bruzzese, P. Manfrinetti, D. Marrè, N. Spinelli, R. Velotta, X. Wang, C. Ferdeghini, presented at *Boromag, Genova, Italy 17-19 June 2002*, in press in *Superc. Sci. Technol.*
11. S.R. Shinde, S.B. Ogale, A. Biswas, R.L. Greene, T. Venkatesan, *cond-mat* **011/0110541**
12. C. Ferdeghini, V. Ferrando, G. Grassano, W. Ramadan, E. Bellingeri, V. Braccini, D. Marré, P. Manfrinetti, A. Palenzona, F. Borgatti, R. Felici, T.-L. Lee, *Superc. Sci. Technol.* **14**, 952 (2001)
13. A. Berenov, Z. Lockman, X. Qi, J.L. MacManus-Driscoll, Y. Bugoslavsky, L.F. Cohen, M.-H. Jo, N.A. Stelmashenko, V.N. Tsaneva, M. Kambara, N. Hari Babu, D.A. Cardwell, M.G. Blamire, *Appl. Phys. Lett.* **79**, 4001 (2001)
14. S.D. Bu, D.M. Kim, J.H. Choi, J. Giencke, S. Patnaik, L. Cooley, E.E. Hellstrom, D.C. Larbalestier, C.B. Eom, J. Lettieri, D.G. Schlom, W. Tian, X. Pan, *Appl. Phys. Lett.* **81**, 1851 (2002)
15. Y. Bugoslavsky, G.K. Perkins, L.F. Cohen, A.D. Caplin, *Nature* **410**, 563 (2001)
16. V. Metlushko, U. Welp, A. Aranson, G.W. Crabtree, P.C. Canfield, *Phys. Rev. Lett.* **79**, 1738 (1997)
17. S.V. Shulga, S.-L. Drechsler, G. Fuchs, K.-H. Müller, K. Winzer, M. Heinecke, K. Krug, *Phys. Rev. Lett.* **80**, 1730 (1998)
18. S.L. Bud'ko, P.C. Canfield, *Phys. Rev. B* **65**, 212501 (2002)
19. Yu. Eltsev, S. Lee, K. Nakao, N. Chikumoto, S. Tajima, N. Koshizuka, M. Murakami, *Physica C* **378-381**, 61 (2002)
20. L. Lyard, P. Samuely, P. Szabo, C. Marcenat, T. Klein, K.H.P. Kim, C.U. Jung, H.-S. Lee, B. Kang, S. Choi, S.-I. Lee, L. Paulius, J. Marcus, S. Blanchard, A.G.M. Jansen, U. Welp, W.K. Kwok, *cond-mat/0206231*
21. G. Blatter, V.B. Geshkenbein, A.I. Larkin, *Phys. Rev. Lett.* **68**, 875 (1992)
22. S.V. Shulga, S.-L. Drechsler, H. Eschrig, H. Rosner, W.E. Pickett, *cond-mat/0103154*
23. S.V. Shulga, S.-L. Drechsler, *Rare Earth Transition Metal Borocarbides: Superconducting, Magnetic and Normal State Properties*, edited by K.-H. Müller, V. Narozhnyi, NATO Sciences Series, **393** (2001)